Yugoslav Association of Metallurgical Engineers *UDC:669.258.67.784.068=20*
YAME

TRANSPORT AND CHEMICAL RATE PHENOMENA OF PLASMA ACTIVATED CVD OF CO-C-O–LAYERS

A. NÜRNBERG[1], R. STOLLE[1], K. T. RAIĆ[2] AND G. WAHL[1],

[1]*Institut für Oberflächentechnik und Plasmatechnische Werkstoffentwicklung, TU Braunschweig, Germany*
[2]*Faculty of Technology and Metallurgy, Belgrade University, Yugoslavia.*

ABSTRACT

Transport and chemical rate phenomena were analysed for Co-C-O-layers generated on steel C35 from cobalt(II) acetylacetonate by PACVD. The investigations were carried out in a parallel plate reactor, under the high frequency (13.56 MHz) plasma, with low ionization (ionization degree 10^{-7}-10^{-6}, electron temperature 5 eV, electron density 0.6 10^{15} to 1.8 10^{15} m^{-3}) and at the pressure of 100 – 400 Pa. Presented coating system was taken as a good example for the plasma activated CVD process simulation.

Keywords: PACVD, Co-C-O-layers, transport and chemical rate phenomena

1. INTRODUCTION

It is well known, that the transport and chemical rate phenomena at low preassures with plasma activated chemical reactions in gas phase are extremely complex. In addition, we have usually the transport phenomena in the slip and/or transition regimes. Nevertheless, the analyses of such situation is possible by semi-theoretical and/or empirical procedures, see e.g. [1-4].

The method of simulation is mainly determined by the Knudsen number ($Kn = \lambda/d$) where λ is the mean free path in the gas phase and d a characteristic length in the reactor. At $Kn < 0.01$ continuum calculations can be applied. At $Kn > 0.01$ slip conditions must be taken into account or molecular gas flow must be calculated [1]. CVD processes operate mostly in the range with $Kn << 0.01$. In this range computer codes are available today which solve simultaneously the Navier Stokes equation, the equations for the energy and the molecule transport [2,3].

Plasma activated CVD processes operate very often in the range $Kn > 0.01$. In addition the role of the plasma complicates the process. This might be the reason that very few calculations of plasma activated CVD processes [4-9] are carried out. In spite of this the interest to simulate plasma processes is very large because simulation facilitates the scale up of the processes.The deposition process in this study is carried out in the pressure range of 100 – 400 Pa and a

characteristic length of 4,3 cm (distance of the plates) that means in a Knudsen number range of Kn < 0.01. Therefore continuum calculations are possible.

Coatings with general stoichiometry CoC_xO_y are of large industrial interest. Here, the Co - C - O - coatings are deposited from $Co(acac)_2$ by the reduction in hydrogen:

$$Co(acac)_2 + H_2 \rightarrow Co + 2H(acac)$$

For atmospheric preassure, the Arrhenius plot of log average Co deposition rate versus inverse of deposition temperatures showed similar deposition rates from 318-352°C [5] 270-310°C [6]; and 270-290°C [7]. This suggested a feed-rate-limited growth mechanism. Also, it was observed in the experiments that deposition rate of Co did not decrease with increasing temperature [7]. On the other hand, sublimation of the the precursor at higer temperatures results in irreproducible deposition rates, perheps because of decomposition of the precursor in the sublimator. It was observed by [6] that volatile organic products formed during the reduction as well as unreacted $Co(acac)_2$ are swept downstream beyond the furnace tube linear and either deposit on the cool furnace wall beyond the tube furnace or are swept further through a thermal conductivity cell.

2. EXPERIMENTAL

A schematic diagram of the RF - deposition equipment and the reactor is shown in Fig.1. All gas flow rates were adjusted by mass flow controllers. The upper electrode (75 mm diameter) was grounded and worked also as a shower for the process gas. The upper electrode was specially constucted and perforated with 1010 holes (diameter 1mm) on the outlet. The lower electrode (the carrier for the substrates) was dc isolated and heated to maximum temperatures of 723K. The temperature of the substrate was measured with a NiCr/Ni thermo-couple, located inside of the lower electrode. Also, the temperature was controlled by an Eurotherm controller. The electrodes were connected via a match box to the RF-generator (Branson / IPC U. S., Model PM-119, 13.56 MHz).

The lower electrode had negative voltages in the range -20 V up to -475 V (self bias) depending on the electric power P. The electric probe for measuring the probe voltage and probe current was positioned in a distance of 8 mm above the lower electrode, outside of the plasma sheath.

The deposition reactor was made of stainless steel. Metal sealings were used. All substrates (19.5 mm diameter) were made of steel (C35), hardened up to Knoop hardnesses of HK0.01 = 600 - 650, polished (surface roughness smaller 1 μm) and ultrasonically cleaned. The precursor $Co(acac)_2$ was delivered from the company STREM. The precursor concentration in the gas phase were determined by the mass change of the crucibles from which the precursors were evaporated. The molar fractions were in the range of $x(Co(acac)_2)= 0.5 - 1$ %.

The deposition reactor was connected with a quadrupol mass spectrometer (1 – 100 amu)

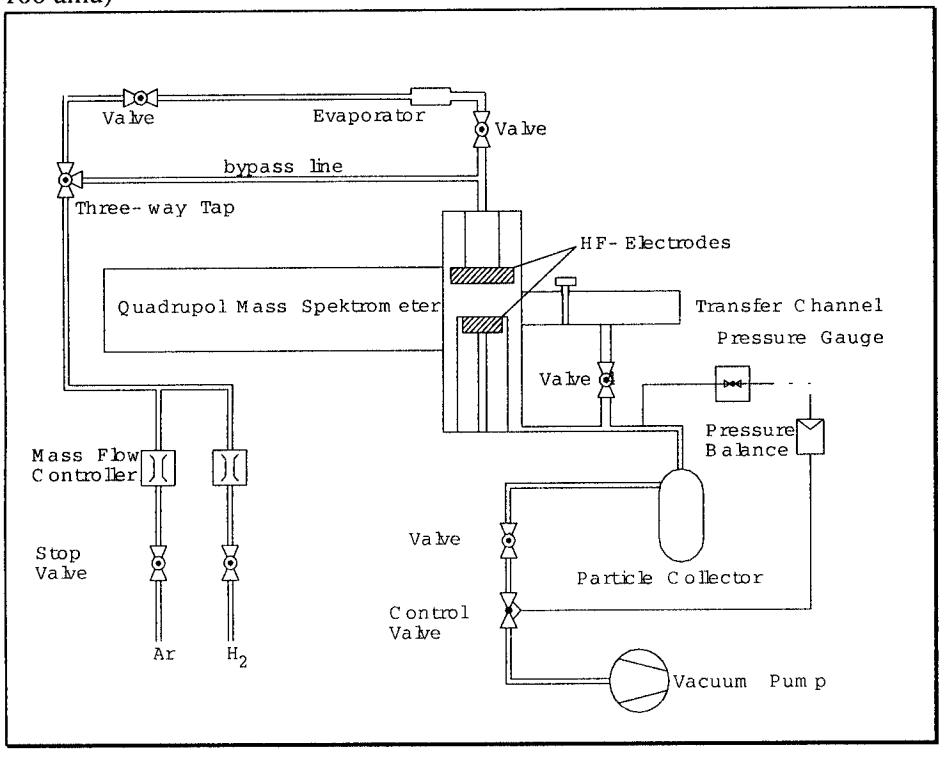

Fig 1a. PACVD equipment

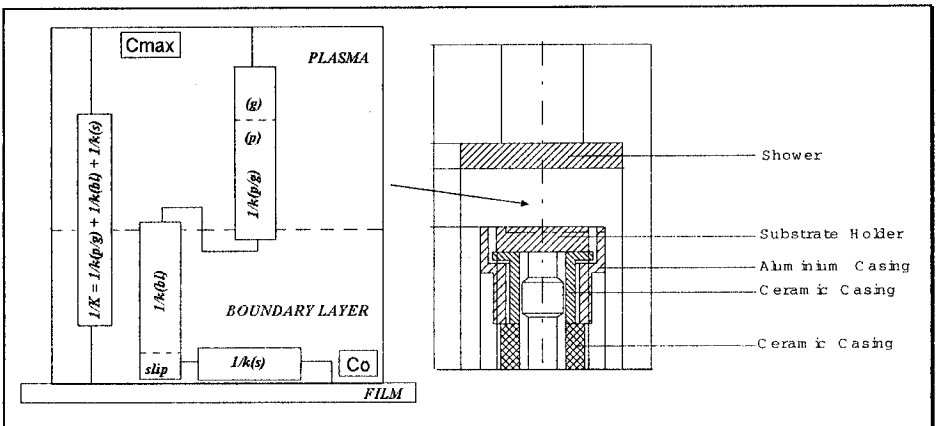

Fig. 1.b. PACVD plate reactor with simplified description of PACVD process

The deposition experiments were carried out with the following procedure: After evacuation of the reactor to 1 Pa the working pressure was adjusted from 100 Pa to 400 Pa whereby the gas was conducted through the bypass line shown in Fig. 1. The ratio of the gas flows Ar(sccm)/H_2(sccm) was kept at 15/35. Feeding pipes, shower (upper electrode) and substrate holder (lower electrode) were heated up to the temperatures: T_{pipe}= 323 K, T_{shower}= 348 K, T_{subst}= 523, 623 and 723 K. The evaporator was heated to the temperatures of $T_{evaporator}$= 390 – 400 K. The RF - power generator was switched on and the power input was adjusted between P = 25 W and P = 150 W. After 30 minutes all parameters were stabile. The bypass (Fig. 1) was closed and the gas flow through the evaporator and the deposition process begun. The mass deposition rates were measured by determination of the mass of the substrates before and after the deposition experiment. Typical deposition times were t = 2 h. The molar deposition rates were calculated by the assumption that pure Co were deposited. The thickness growth rates were calculated with the densitiy of Co (8.8 g/cm^3)

The composition of the layers was determined by wave length dispersive X-ray analysis (WDX) analysis and the crystal structure by X-ray diffraction. The mechanical properties were determined by the measurement of the Knoop hardness HK0.01. Typical layer thicknesses for these measurements were 1-2 μm.

The electrical measurements were carried out with a directly heatable and an indirectly heatable Langmuir probe. The first probe could also be used as a mass detector for negatively charged particles. In this case the measurements were carried out in the afterglow where the electrons were adsorbed on particles and walls and no free electrons existed in the gas phase.

3. RESULTS OF CO-C–O DEPOSITION

All coatings deposited by this method contained C and O. The general stoichiometry of the coatings could be described by the formula CoC_xO_y with x ~ 0.5 and y = 0.1 – 0.2

The power dependence of the deposition rate with the temperature as parameter is shown in Figure 2. The scattering of the measuring points in the figures is mainly caused by the scattering of the precursor molar fraction in the gas phase. The scattering was in the range of ±20%. In this figure the diffusion controlled deposition rates are plotted also as described in the last section for every deposition condition. The simulated rates are larger than the measured rates and no temperature dependence and no power dependence is found in the calculations In contrast to this the experimental curves for 200 and 400 Pa show no power dependence above a threshold power P_{thr} and at large pressures. At other conditions the deposition increases almost linearly with the power. The threshold power P_{thr} is defined as the power where 80 % of the saturation value

is reached. This threshold power has the values: P_{thr} ~ 40 W for p=400 Pa, P_{thr} ~ 90 W at 200 Pa. In addition there is a deposition at no plasma and all deposition rates are temperature dependent.

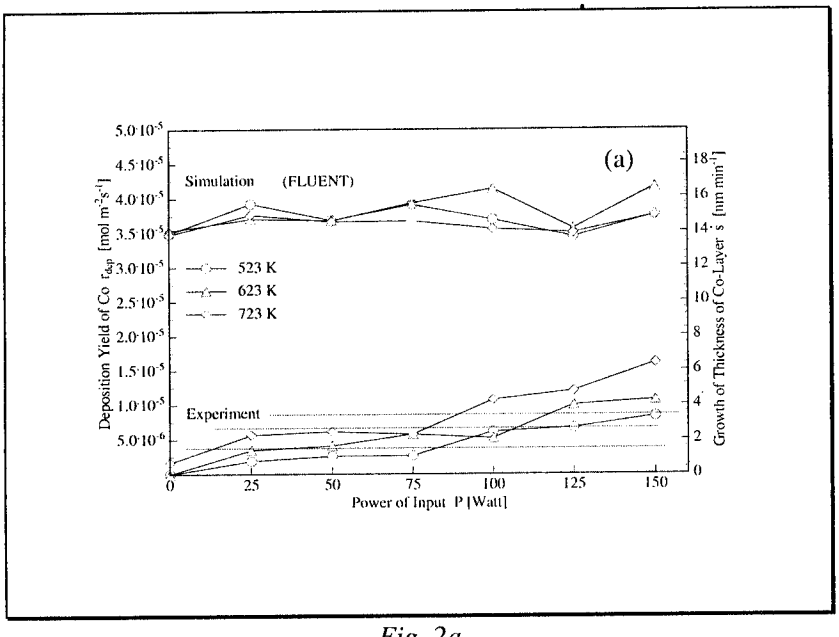

Fig. 2a

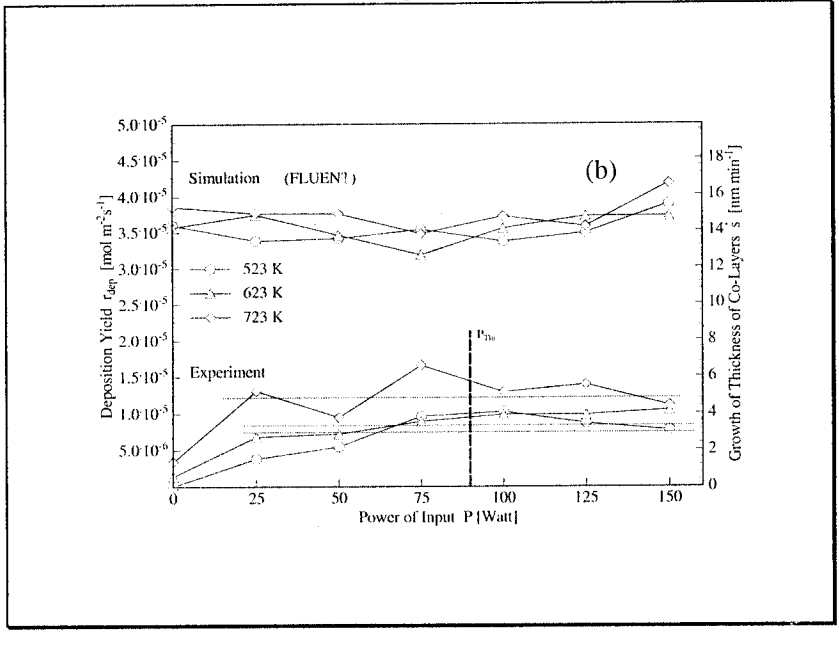

Fig. 2b

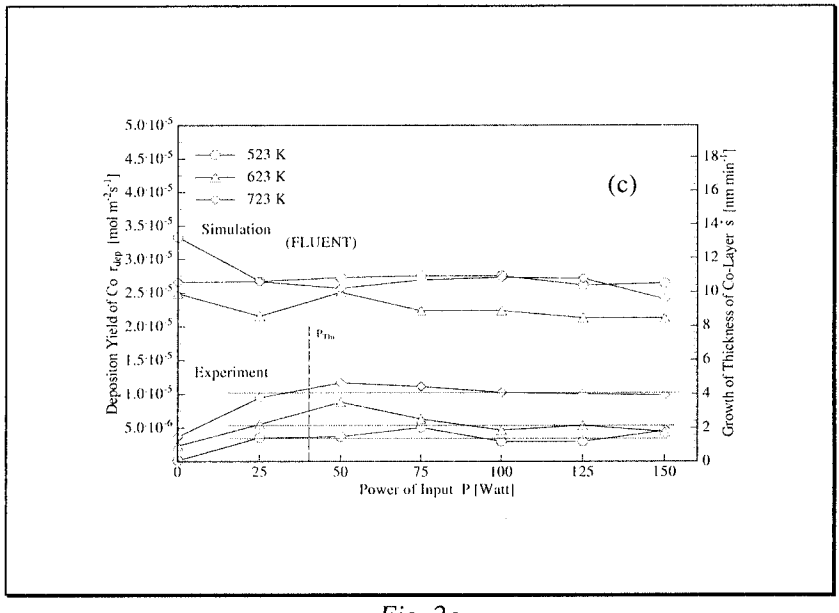

Fig. 2c

*Figure 2 - Estimated and measured deposition rates vs the RF-power P. Substrate temperatures: 523 K, 623 K, 723 K; total pressures: (a) 100 Pa; c(Co(acac)$_2$): 1.1-1.3*10^{-4} mol m^{-3}; (b) 200 Pa: 2.3–2.6 10^{-4} mol m^{-3}; (c) 400 Pa 3.0-23.3 10^{-4} molm^{-3} Flow: Ar: 15sccm, H_2: 35 sccm*

4. ELEMENTS OF PROCESS MODELLING

4.1. Fluid Dynamics

Configuration of the reactor (Figure 1) enables the good description of the momentum, heat and mass transport as well as chemical rate phenomena. We have an example of exact solution of the Navier-Stokes equations: ***stagnation in three–dimensional flow***. A fluid stream impinges on a wall at right angles to it and flows away radially in all directions /the axisymmetric case/. There is a flow parallel to its axis in the neighborhood of a stagnation point of a body of revolution (substrate). The velocity distribution in frictionless potential flow in the neighborhood of the stagnation point at r = z = 0 is given by: U = ar and V = az, where a denotes a hydrodynamic constant (U the velocity at the boundary layer core).

The solution of the appropriate differential equation was first given by F.Homman [11] in the form of a power series. If we consider the corresponding distance from the wall, denoted by $z = \delta_v$ as the boundary layer, we have: $\delta_v \cong 1.98(\nu/a)^{1/2}$ [N. Frossling, 1940]. The layer is small at low kinematic viscosities and proportional to $\nu^{1/2}$. It is worth noting that the dimensionless velocity distribution u/U in the boundary layer as well as the boundary layer thickness are independent of r coordinate.

For practical application the hydrodynamic constant, a, must be known. Here, the solution taken from analysis of mass transfer to an impinging electrode [14] is used:

$$a^* = ad_{eq}/V^* = 1.5129H^{*-0.204} \qquad (1)$$

wher: d_{eq},equivalent nozzle diameter, V*, average nozzle exit velocity, H* = H/d, dimensionless nozzle heigh, H nozzle heigh.

Configuration of the upper two-stage shower is designed to achive a better uniform deposition on the substrate. The outside shower is perforated with 1010 holes (diameter 1 mm). This is a type of flow control device (FCD) used for modifying the flow inside the PACVD reactor (A simple design for an FCD may be a round plate with holes in concentric rings on it). Various designs of FCDs are possible. Hole size and distribution on the plate may be optimized by using the computor code as well as experimental data. A careful optimization of hole radii and plate thickness can provide a perfect homogeneity at the gas inlet. Our type of shower enables an uniform boundary layer thickness at low preassures.

4.2. Heat Transfer

Relatively low temperatures of "shower" (348 K) and substrate (523, 623 and 723K) indicate the pure forced convection heat transfer from substrate toward plasma. Radiation heat transfer is minor. So we have the usual relationship (similar and analogous to eq. 5):

$$Nu = C\, Re_r^{1/2}\, Pr^{1/3}$$

$$(Nu = hr/\lambda,\ C \approx 1,\ Re_r^{1/2} = Ur/\nu,\ Pr = \nu/\alpha,\ \alpha = \lambda/\rho cp,\ \delta_v/\delta_T = Pr^{-1/3})$$

Thermal effects of the deposition, like the latent heat of sublimation, can be added to the total energy balance. Also, thermal instabilities on the "shower" caused by electro-magnetic effects might be taken into the consideration. It is possible to implement this effecs into the presented calculations.

4.3. Mass Transport and Chemical Rate Phenomena

Plasma activated chemical vapor deposition (PACVD) is the complex phenomena involving thermodynamics, reaction rates, convection patterns and mass transfer in systems that are nonisothermal and far from equilibrium. Also, the plasma reactions can be extremely complex and multifold.

In order to illustrate the role of the transport and chemical rate phenomena in the film forming, a relative simple situation will be considered, with the chemical reactions in the plasma/gas phase, diffusion through the boundary layer over the film and finally, chemical reactions at the film surface (Figure 3). The flux through the plasma/gas, the flux through the boundary layer and the film surface reaction flux are all equal. In other words, it is a typical steady-state process with uniform flux, analog to three resistences in series (1/K) and an overall potential of ΔC = (Cmax - Co).

It must be mentioned that because of very thin film (1-2μm) we can neglect the effects of diffusion through the solid film as well as phenomena at film/substrate interface.

So, generally, we can describe our PACVD process with following simultaneous sub-processes:

(1) homogeneous chemical reactions and phenomena in the plasma/gas (plasma assisted and pure CVD chemical reactions) [**k(p/g)**],
(2) diffusion through the boundary layer (with/without slip effect) [**k(bl)**] and
(3) heterogeneous chemical reactions and phenomena on the solid substrate [**k(s)**];

unknowing the real influence of each on another. Simplified presentation of the PACVD is given on the Figure 1.

The rate of film growth (j) is given as:

$$j = \Delta C/[1/k(p/g)] + [1/k(bl)] + [1/k(s)] = K\Delta C,$$

$$K = 1/[1/k(p/g)] + [1/k(bl)] + [1/k(s)] \qquad (2)$$

where, ΔC = (Cmax - Co) is an overall potential, Cmax: the precursor concentration under the upper electrode (shower), Co the precursor concentration above the substrate (in some cases Co = 0) and K: the overall transport coefficient
On the other hand, the flux of adding active molecules from the gas to the film of thickness δ_f, is:

$$j = (\rho/M)d\delta_f/dt \qquad (3)$$

or the deposition rate is:

$$d\delta_f/dt = (M/\rho)\, K\Delta C \qquad (4)$$

where, ρ: the density of Co and M: the mass of Co per molecule.

The rate of film growth (j) does not always correspond to the rate of precursor disappearance (J). Because of reactor simple geometry and only one effective deposition we can assumed that j = J. In another words, there no exist more parallel deposition processes but only one.

Often, depending on the deposition regime, one of the processes becomes the most important and we have:

(I) plasma/gas phase reactions and phenomena, [**j = k(p/g)** ΔC];
(II) diffusion through the boundary layer, [**j = k(bl)** ΔC] and
(III) surface reactions and phenomena, [**j = k(s)** ΔC],
limited process.

We must know, there is a domain in which none of the processes dominates, so the overall PACVD cannot be simplified.

In our simulation we analyzed the PACVD as the laminar transport phenomena during homogeneous/heterogeneous appearances in the neighborhood of substrate surface. Deatails of this concept was pubished in [8-10]. It means, that the diffusion through the boundary layer is the referent situation. So, the starting position for the calculation is the usual correlation:

$$Sh = C\, Re_d^{1/2}\, Sc^{1/3}, \qquad (5)$$

$$(Sh = \beta d/D,\ C = 0.85\, a^{*1/2} \approx 1,\ Re_d^{1/2} = Ud/\nu,\ Sc = \nu/D)$$

Note, that the boundary layers thicknesses (δ_ν, δ_T and δ_C) are independent of r coordinate ($\delta_\nu/\delta_C = Sc^{-1/3}$ and $\delta_\nu/\delta_T = Pr^{-1/3}$).

5. SEMI-THEORETICAL CONCEPT OF LAMINAR BOUNDARY LAYER

Because of well defined dimensions of reactor, the laminar boundary layer concept is proposed for modelling the coupled transport phenomena [8-10].

Integral methods, based on setting balances for the control volume, are often used in practice for the cases of laminar boundary layer [11-13]. The well known problem in the application of these methods is the definition of satisfactory equations for the concentration distribution. According to the literature data, the use of a certain distribution equation is most commonly limited to the corresponding specific system. When the conditions are changed, it is necessary to choose a new, more appropriate distribution equation. In order to overcome this situation, an ordinary differential equation, the ***"simplified"*** equation is proposed. Solution of this equation, normalized concentration distribution θ, is considered in the most general sense of term with analogous meaning for momentum, mass, heat, chemical reaction, electro-magnetic forces etc.. For example, momentum, analogous to concentration, by its distribution in the laminar boundary layer, forms a corresponding **F**lux **G**radient (FG). Accordingly, a heterogeneous/surface appearance (i.e. chemical reaction) can be considered as a phenomenon of concentration change with the corresponding distribution and FG.

For appropriate situation of PACVD: (i) homogeneous appearances are present inside a gas/plasma phase (i.e. pressure gradient, homogeneous chemical reaction, electro-magnetic forces, plasma etc.) and (ii) heterogeneous appearances are present on surface of substrate (i.e. condensation, heterogeneous chemical reaction, surface heterogeneities, etching etc.).

So, the ***"simplified"*** equation defines the **F**lux **G**radient (FG-code) of the concentration change phenomena

$$FG = {}_i\int^0 \theta''\, d\xi = N + f(m)\ ; \quad N \in [0, 2]\,, \quad f(m) \in [0, \pm\infty] \qquad (6)$$

In principle there are laminar layers with:

- constant FG along the referent axis (FG = N; f(m) = 0), i.e. the laminar boundary layer over a flat plate or rotating disk and here, stagnation in three–dimensional flow.
- variable FG, i.e. laminar entrance region flow, when every position has its corresponding distribution.

The modelling procedure of complex systems with simultaneous sub-processes, is reduced to the constitution of balances of FG-codes of the

phenomena occurring within a system. Momentum flow (υ) is the "promoter" of the whole heat and/or mass transport. By its velocity distribution along the interphase it produces a FG-code which induces identical behavior of the thermal and/or diffusion processes in fluid. Heterogeneous appearances easily embarrasses the heat/mass transport process. So, for diffusion (D) during heterogeneous appearances (H) over the flat plate, when temperature is constant or slightly variable:

$$FG_{\upsilon}dx = (FG_D \pm FG_H)dx \qquad (7)$$

According to balance equation (7), referent situation:

$$N_{\upsilon}dx = N_D dx \qquad (8)$$

and simplified analysis of Frank-Kameneskii [13]

$$k^*Co = \beta(Cmax - Co) \qquad (9)$$

the model of mass transfer coefficient

$$\beta = k^*(Co/Cmax)/(1 - Co/Cmax)\{1/1 - [\pm f(m)_{\upsilon} \pm f(m)_D \pm FG_H]/N_{\upsilon}\} \qquad (10)$$

and/or dimensionless surface concentration ratio

$$Co/Cmax = 1/\{1 + z[1 - (\pm f(m)_{\upsilon} \pm f(m)_D \pm FG_H)/N_{\upsilon}]\};\ z = k^*/\beta \qquad (11)$$

are developed.

So, for $[1 - (\pm f(m)_{\upsilon} \pm f(m)_D \pm FG_H)/N_{\upsilon}] = \Phi$ (numerical value of real conditions) one can obtained

$$j = \beta\Delta C/(1 + (z\Phi)^{-1}) \text{ or } d\delta/dt = (M/\rho)\beta\Delta C/(1 + (z\Phi)^{-1}) \qquad (12)$$

Influence of $f(m)_{\upsilon}$ on the dimensionless surface concentration Co/Cmax for a first order reaction and balance $[N_{\upsilon} \pm f(m)_{\upsilon}]dx = N_D dx$ was presented in [8-10] Influence of FG_H on the dimensionless surface concentration Co/Cmax for a first order reaction and balance $N_{\upsilon}dx = (N_D \pm N_H)dx$ constituted over a heterogeneous surface of foil was presented in [8-10], too.

6. VERIFICATION

6.1. Calculations /Procedure and Results [19]/

To find (ΔC) we used the following calculating sequences:

(1) Dependences of dynamic viscosity (μ) on temperature (T) for pure Ar and H_2 are taken from standard handbooks.

(2) Viscosity of gas mixure (15 sccm Ar/35 sccm H_2) is calculated according to the method of Wilke [15].

(3) Density of mixure for various temperatures, T (523, 623 and 723K) and preassures, P (100, 200, 400 and 10^5 Pa) are calculated simply as: $\rho = P/((RT\Sigma(w_i/M_i))$; where: w_i is the mass fraction and M_i the molar weight of Ar (i=1) and H_2(i=2)

(4) The binary diffusion coefficient of $Co(acac)_2$ in pure H_2 is calculated according to the formula [15]: $D_{AB} = 0.00266T^{3/2}/(PM_{AB}^{1/2}\sigma_{AB}^{2}\Omega_D)$; where: D_{AB} is binary diffusion coefficient, cm^2/s; T temperature, K; P pressure,

bar; σ_{AB} characteristic length, Å; Ω_D diffusion collision integral, dimensionless. Lennard-Jones parametes used in calculations are listed in [19].

(5) Criteria's of Re, Sc and Sh are estimated from usual relationships and listed in [19], with appropriate boundary layer thicknesses as well as mass transfer coefficients.

(6) Values for ΔC (overall potential of the precursor) for averaged deposition rates data, are listed in [19] and traced into the Figures 2a,b and c.

(7) With Φ (numerical value for real condition) one can modified the deposition rate taken from (6). Φ might be the function of some plasma property and/or power of RF generator.

By this technique an analytical relationship between j, ΔC and r can easily be obtained.

6.2. Simulation /Double Contol/ by Fluent®

For the double control simulation calculations the reactor shown in Figure 2 was simplified and the computer code Fluent® was used. The form is axisymmetric, which simplifies the deposition calculations to a two dimensional calculation with the z axis and the radius as additional coordinate. For the calculation of the gas flow and the deposition rate the grid consisted of 1830 cells, 30 cells in the radial direction corresponding to 50 mm internal radius and 61 cells corresponding to 265 mm in height. The viscosity and the heat conductivity of the gas mixture were calculated according to the codes given in Fluent.

7. CONCLUSION

In the system W - C - O the deposition is strongly influenced by a particle formation in the gas phase. Inspite of the vacuum sealed equipment the layers always contain oxygen. The activated molecules are formed during the flowing of the molecules from the shower to the substrate. Therefore the oxygen comes from the precursor compounds. The deposition temperature is rather low, the maximum temperature is 750 K. Because of these reasons, the PACVD deposition of Co - C – O layers is discussed in the light of transport and chemical rate phenomena at low preassures with plasma activated chemical reactions in gas phase.

The presented concept is imagined as a flexible iterative system for the following experimental data. The model can be used as a tool in computer-aided process optimization, too. Therefore, in second step, the standard numerical methods (statistics as well as interpolation procedures) must be used as superstructure.

Acknowledgement

The authors thank for the Deutscher Akademischer Austauschdienst (DAAD) support on the cooperation between Prof. Karlo T. Raić and Institut für Oberflächentechnik und Plasmatechnische Werkstoffentwicklung, TU Braunschweig, Germany.

REFERENCES

[1] Rhee, S., Szekeley, J., J. Electrochem. Soc.: *Solid-State Science and Tec-hnology,* (1986), Vol. 133, No. 10, 2194 – 2201
[2] Kushner, M. J., *J. Appl. Phys.* **63** (8), (1988)
[3] Spence, R. J., Thesis (Ph. D.) Univ. Arkansas, Fayetteville, AR, USA, 1993
[4] Gladush, G. G., Rodionov, N. B., *J. Chem. Vap. Deposition* (1997), 6(1), 76 -83
[5] Jablonovski, *J., Cobalt,* 28 (14) (1962)
[6] Charles, R. G. and Haverlack, P. G, *J. Inorg. Nucl. Chem.*, 995(31) (1969)
[7] Gu, S. et al, *Thin Solid Films*, **45** (340) (1999)
[8] Raic, K. T., *ISIJ Int.*, 1992, **32,** 514-520.
[9] Raic, K. T, *J. de Physique IV*, C5, 1995, **5,** 235-242.
[10] Raic, K. T., *Interface Science*, 85 (8) (2000)
[11] Schlichting, H., *Boundary-Layer Theory*, Pergamon Press, New York, 1955.
[12] Bird, R. B, Stewart W. E. and Lightfoot, E. D., *Transport Phenomena*, John Wiley and Sons, New York, 1960.
[13] Frank-Kamenetskii, D. A., Diffusion and Heat Exchange in Chemical Kinetics, Princeton University Press, Princeton, 1960.
[14] Chin, D-T. and Tsang, C-H., *J. Electrochem.Soc.:Electrochemical Science and Technology*,(1978) p.1461-1470
[15] Reid, R. C., Prausnitz, J.M. and Poling, B. E., The Properties of gases and liquids, McGraw-Hill Book Co., New York, 4th edition, 1987
[16] Laidler, K. J., Chemical Kinetics HarperCollins, New York 1987
[17] Metals and Alloys, JCPDS-International Centre for Diffraction Data
[18] K. H. Habig Verschleiß und Härte von Werkstoffen, Carl Hanser Verl. 1980
[19] Arnold Nurnberg, A., Stolle, R., Wahl, G. and Raic, K., CIMTEC 2002, Florence, Italy, 2002 (full text will be published in the 10th Ceramics Congress Monographs, 2003).

NOMENCLATURE

a : hydrodynamic constant; Co : surface concentration; C_{max} (=$C_{\xi=1}$ when f(m) = const, or f(m) = 0,) : theoretical bulk/core concentration; d : diameter; D : (binary) diffusion coefficient; FG : Flux Gradient (FG-code); FG_D : the diffusion flux gradient; FG_H : flux gradient of the total heterogeneity; k* : (heterogeneous chemical reaction) rate constant according to [13]; N : dimensionless criterion; Nu : Nusselt number; Pr : Prandtl number; R : gas constant; Re : Reynolds number; r, z : coordinates; Sc : Schmidt number; Sh : Sherwood number; T : temperature; V, U : velocitis in r and z directions; V* : average nozzle exit velocity.

Greek symbols

α : thermal diffusivity; β : mass transfer coefficient; δ_C : concentration boundary layer thickness; δ_T : temperature boundary layer thickness; δ_v : kine-matic boundary layer thickness; δ_f : deposited film thickness; $\xi = y/\delta$: dimen-sionless distance from interphase; ν : kinematic viscosity; μ : dynamic visco-sity; $\theta = C/C_{\xi=1}$: normalized concentration distribution; $\theta'' = d^2\theta/d\xi^2$: derivation of second order.